Cold Start of a Radiator Equipped with Titanium-Water Heat Pipes

Donald A. Jaworske[1]
NASA Glenn Research Center, Cleveland, Ohio, 44135

James L. Sanzi[2]
Sest Inc., Middleburgh Heights, Ohio, 44130

and

John Siamidis [3]
NASA Glenn Research Center, Cleveland, Ohio, 44135

Radiator panels utilizing titanium-water heat pipes are being considered for lunar applications. A traditional sandwich structure is envisioned where heat pipes are embedded between two high thermal conductivity face sheets. The heat pipe evaporators are to be thermally connected to the heat source through one or more manifolds containing coolant. Initial radiator operation on the lunar surface would likely follow a cold soak where the water in the heat pipes is purposely frozen. To achieve heat pipe operation, it will be necessary to thaw the heat pipes. One option is to allow the sunlight impinging on the surface at sunrise to achieve this goal. Testing was conducted in a thermal vacuum chamber to simulate the lunar sunrise and additional modeling was conducted to identify steady-state and transient response. It was found that sunlight impinging on the radiator surface at sunrise was insufficient to solely achieve the goal of thawing the water in the heat pipes. However, starting from a frozen condition was accomplished successfully by applying power to the evaporators. Start up in this fashion was demonstrated without evaporator dryout. Concern is raised over thawing thermosyphons, vertical heat pipes operating in a gravity field, with no wick in the condenser section. This paper presents the results of the simulated cold start study and identifies future work to support radiator panels equipped with titanium-water heat pipes.

Nomenclature

cm	=	centimeter
m	=	meter
T	=	temperature, K
W	=	watts

I. Introduction

Radiator technology risk reduction is part of the Heat Rejection System effort for Fission Surface Power and as part of the risk reduction activities, Glenn Research Center procured three Radiator Demonstration Units (RDU's). Each RDU consists of a composite honeycomb sandwich radiator panel with embedded titanium-water heat pipes. The performance of the three as-delivered RDU panels was evaluated in early 2007 and a paper summarizing the test results was presented.[1] In the previous work, panel performance was evaluated in a vacuum chamber equipped with liquid nitrogen (LN2) cold walls at the following steady state thermal inputs: 200, 300, and 350 watts per heat pipe. Simulated micrometeoroid impact with loss of a heat pipe, and freeze/thaw conditions,

[1] Physicist, Space Environment and Experiments Branch, 21000 Brookpark Rd., Cleveland, Ohio, AIAA Member.
[2] Heat Transfer Engineer, Thermal Energy Conversion Branch, 21000 Brookpark Rd., AIAA Member.
[3] Thermal Systems Engineer, Thermal and Fluid Systems Analysis Branch, 21000 Brookpark Rd.

were also evaluated. Not evaluated in 2007 was the panel performance under 1 sun illumination, including the effect of illumination on panel start after freezing the water in the heat pipes, and the effect of illumination on steady state temperatures with heater power applied. The objective of this paper is to evaluate panel performance under 1 sun illumination.

II. Illumination

To address the goal of evaluating the performance of the RDU panels under 1 sun illumination, the vacuum facility used previously was equipped with four 1 kW lamps, with reflectors, capable of producing more than enough radiant energy to meet the 1.38 kW/m^2 needed to simulate 1 sun. Figure 1 shows a panel and the lamps installed in the vacuum facility. Quartz halogen lamps were selected for economy. It should be noted that quartz halogen lamps do not simulate the spectral intensity of the sun, indeed, they provide a spectral intensity weighted in the infrared. It should also be noted that the RDU panels are unpainted and have optical properties weighted in the infrared. Hence, as part of this work, it was necessary to adjust the lamp intensity to simulate the radiant energy exchange between 1 sun and a panel coated with a low absorbing optical coating by utilizing a radiant source emitting heavy in the infrared and an uncoated panel having a high absorptance. This was achieved by incorporating the spectral output of the lamps and the spectral optical properties of the as-manufactured RDU panel.

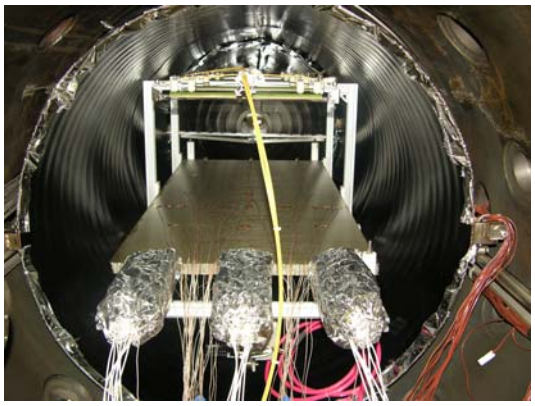

Figure 1. Framework above the RDU panel holding four quartz halogen lamps.

A beam survey was conducted to identify lamp intensity as a function of location prior to testing. The results of the beam survey are included here:

1) The spectral output of the lamps were measured utilizing a sample of Spectralon® placed on top of the panel to provide a Lambertian surface and the reflected light was measured by a FieldSpec® spectroradiometer in the wavelength range of 350 – 2500 nm, the limits of the instrument. Lamp output was assumed to be sufficiently consistent for the purpose of these tests.
2) A curve fitting program was used to established a calculated output over the wavelength range of 350-5000 nm.
3) The area under the calculated output curve was summed yielding total illumination energy, in W/m^2.

Figure 2 shows an example of the measured spectral data and the calculated output curve over the wavelength range of 350-5000 nm. The area under the curve represents total intensity, and in this example the total area under the curve is 354 W/m^2.

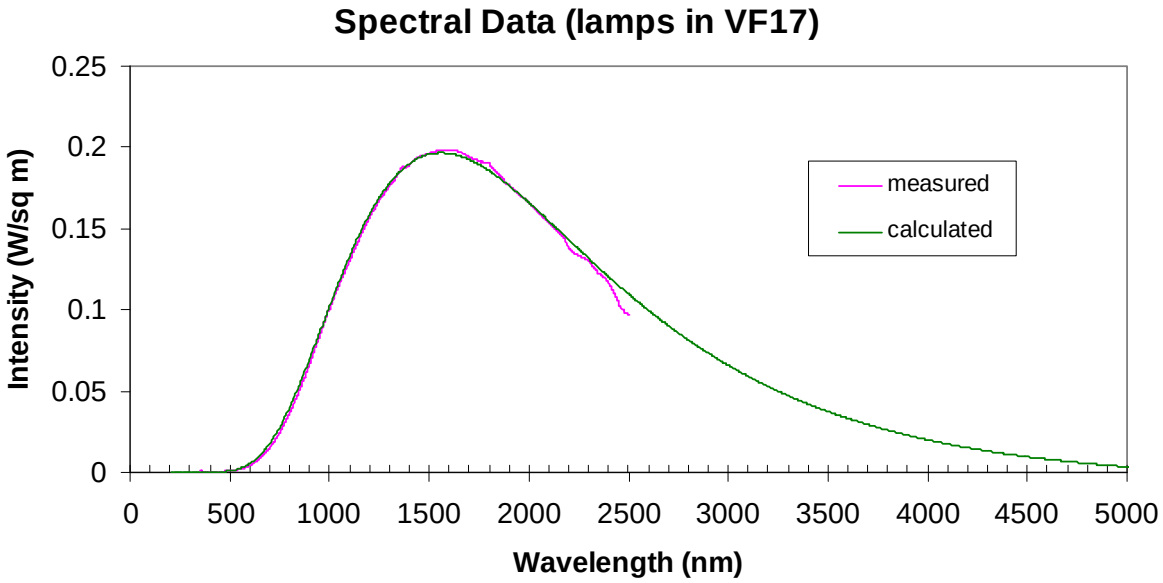

Figure 2. Measured and calculated spectral data.

Lamp intensity was measured at several locations on the panel and at several lamp intensities as dialed in by the lamp power supply rheostat. The results are summarized in Figure 3.

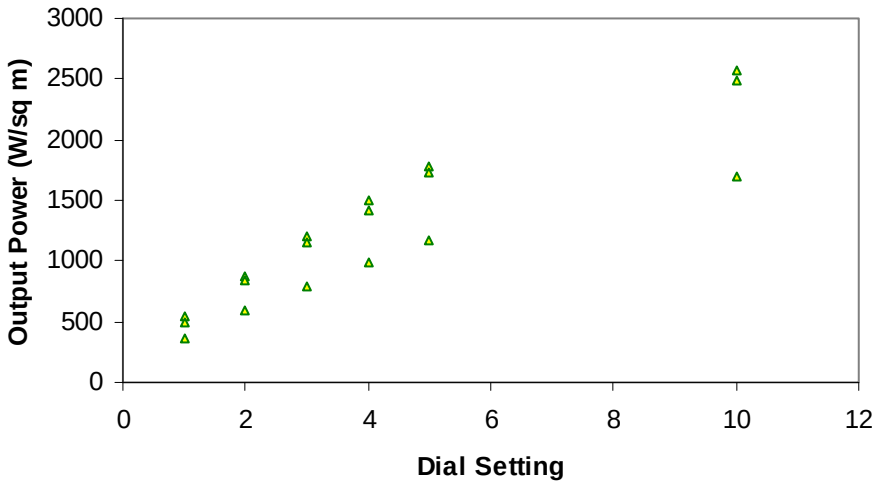

Figure 3. Output Power versus Rheostat Dial Setting.

Over the rheostat settings of 0 to 5, the lamp intensity was found to be linear, with the intensity saturating prior to a rheostat setting of 10. Summations under the curves yielded a 1 sun value, in terms of W/m^2, at a rheostat setting in the vicinity of 4. (The values at a rheostat setting of 4 in Figure 3 are 1506.7, 1425.0 and 983.3 W/m^2.) This span of values was found to be consistent with the areal survey, as discussed below.

An areal survey was conducted across the length and width of the panel utilizing a thermopile embedded in an aluminum disk. Figures 4 and 5 summarize the span in intensities over the length and width of the panel at different positions, with the lamp positions highlighted in blue. Interestingly, the intensity down the length of the panel was greatest at the region between the lamps rather than under each lamp, owing to the gold-coated reflectors used above each lamp. The large variability in intensity across the width of the panel is brought about by the length of the filament in the lamp and its corresponding temperature gradient.

These data were transcribed into the vacuum facility thermal model for subsequent use. From the data, it was decided to accept that a rheostat setting of 4 was "equal" to 1.38 kW/m^2. To accommodate the lack of a thermal control coating on the panel it was necessary to reduce the lamp intensity to 20% of 1 sun in order to represent a solar absorptance of 0.2 a typical solar absorptance value for white thermal control paint. Hence, to simulate 1.38 kW/m^2, the rheostat was set at 0.8 for 1 sun testing. To bracket the 1 sun testing and to provide a worst case scenario, it was also decided to conduct testing at 1.5 suns, i.e. a rheostat setting of 1.2.

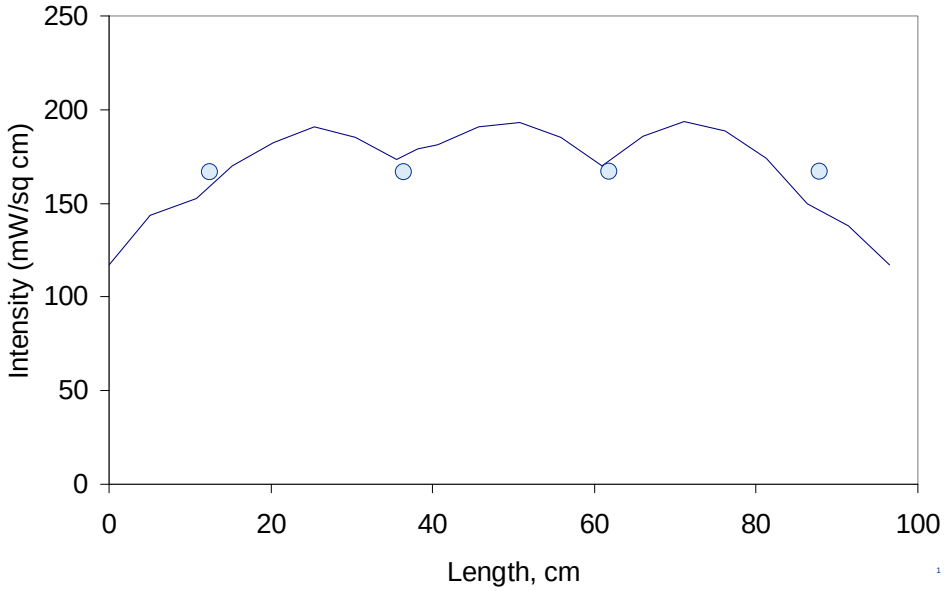

Figure 4. Intensity down the length of the panel.

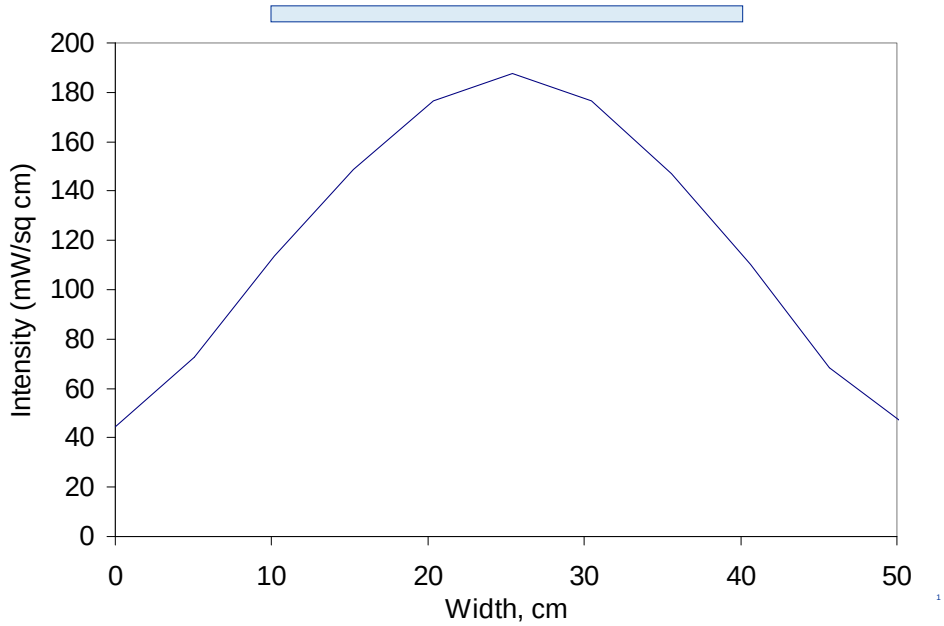

Figure 5. Intensity across the width of the panel.

III. Radiator Panels

The RDU panels are described in detail elsewhere.[1] Briefly, they are flat panels approximately 2.54 cm thick by 0.5 m wide and 1 meter long. High thermal conductivity carbon-polymer face sheets are adhesively bonded to an aluminum honeycomb core and three titanium-water heat pipes are embedded within the core to provide heat transport. The heat pipes are adhesively bonded to a graphite foam saddle and the foam is in turn bonded to the PMC face sheets for the purpose of simultaneously providing a thermal pathway and addressing mismatch in coefficients of thermal expansion. Thermal resistance incurred through the graphite foam saddle and adjoining adhesive layers was found to be somewhat disappointing owing to the adhesive and low areal density of contact.[1]

The graphite fiber selected for construction was K13D2U from Mitsubishi. Although the graphite fiber was common to all three panels, different materials were used for the polymer matrix and adhesive, including, NASA-developed 6F-polyimides with a phenylethynyl endcap (HFPE), Cytec 5250-4 bismaleimide (BMI), and Bryte EX 1551 cyanate ester. Two of the panels used solid-groove heat pipes. One of the panels used heat pipes having grooves constructed of fine sintered titanium powder metal. Table 1 summarizes the panel construction as well as the panel emissivity as measured by a Surface Optics Corporation portable infrared spectrophotometer.

Table 1. RDU panel properties.

Panel	Heat Pipe	Resin	Adhesive	Emissivity, 375 K	Emissivity, 500 K
A	Machine Groove	HFPE	5250-4 BMI	0.790	0.798
B	Machine Groove	5250-4 BMI	5250-4 BMI	0.819	0.822
C	Powder Metal Groove	EX 1551 Cyanate Ester	EX 1551 Cyanate Ester	0.793	0.802

The heat pipes were manufactured by Advanced Cooling Technologies, Lancaster, PA. Heat pipes were fully tested prior to integration into panels, including thermal performance testing and hydrostatic pressure testing. Sufficient margin was provided in the heat pipe to withstand the vapor pressure of the working fluid at the maximum expected operating temperature of 530 K. At this temperature, internal vapor pressure is 4.6×10^5 Pa. Assembly of the panel constituents was accomplished utilizing a vacuum bagging process at ATK Space Systems, San Diego, CA.

Also common to all three RDU panels was power and thermocouple instrumentation. The RDU panels were powered by cartridge heaters embedded in heater bocks surrounding each evaporator, each heater block capable of supplying 1400 watts of power. Care was taken to wrap the heater blocks in Kaowool™ and multilayer insulation to minimize heat loss. Sixty-nine type T thermocouples were placed at strategic locations across the face of the panel, on the titanium heat pipes at either end of the condenser section, and on the evaporators. All power and thermocouple instrumentation was monitored by a programmable logic controller, with data output sent to an Excel spreadsheet.

IV. Results and Discussion

The goals of testing the RDU panels under illumination are as follows:

(1) Obtain steady-state performance characteristics of the panel to simulate cold start, sunrise, and sunset, by heating the evaporator with cartridge heaters and/or heating the panel with quartz lamps.

(2) Utilize the steady-state performance characteristics as an input to the thermal model in order to tie model performance to as-measured performance. Once validated, exercise the model to understand differences in performance under different operating conditions.

To achieve these goals, three RDU panels were individually tested under thermal vacuum at a temperature not exceeding 530 K. Cartridge heaters attached to each heat pipe provided heat to the evaporator of the heat pipe, simulating heat received from the coolant loop of a power conversion system. Quartz lamps above the panel provided illumination simulating solar illumination. The panel radiated to the LN2 cold wall of the thermal vacuum chamber to simulate heat rejection to space. Power into the heat pipes was measured as well as the resultant RDU panel, heat pipe, and facility LN2 cold wall temperatures.

A. Steady-State Modeling

The panels were evaluated at steady-state according to a test plan and a previously developed thermal model was modified. Thermal Desktop® was utilized to create the in-house model. Power was applied to the lamps to generate 1 sun and 1.5 suns, as defined above, and power was applied to the evaporators at 0, 200, 300, and 350 watts. For each combination of illumination and evaporator power, steady state was reached and thermocouple data were collected. Table 2 summarizes the test numbering scheme. The thermocouple data were ultimately utilized to calibrate the updated thermal model. The model was updated by adding lamp nodes. No other changes were made to the previously verified thermal model. In essence, the power supplied to the lamp nodes in the model was adjusted until data from specific heat pipe and face sheet nodes in the model matched data from strategically placed thermocouples on the panel heat pipes and face sheets.

Table 2. Test number as a function of illumination and evaporator power

	0 Watts	200 Watts	300 Watts	350 Watts
1 sun	Test # 1	Test #3	Test #4	Test #5
1.5 suns	Test #2	Test #6	Test #7	Test# 8A and 8B

Table 3 summarizes the test results from panel B. Figure 6 summarizes the thermocouples referenced in Table 3. The lamp nodes in the model have a lamp power in. This power in was the only parameter adjusted in the updated system model. The lamp nodes also have a lamp power out. Average test heat pipe (HP) power was the electrical power provided to each heat pipe evaporator in the test. Heat pipe power loss through conduction down the wire and through the insulation was known to be 10% from a previous study.[1] Average analysis heat pipe power was the wattage applied to each heat pipe evaporator in the model. RDU maximum temperature is the maximum temperature generated by the model. It is the RDU maximum temperature that was matched to heat pipe thermocouple 16 by adjusting lamp power to the lamp nodes. Thermocouples (TCs) 39, 25, and 11, at strategic locations on the panel face sheet, were matched to nodes in the model. From this test plan process, two conclusions were drawn. First, to match the thermocouple data, the four lamp nodes in the model each provided 50 and 66.6 watts of power to the panel at 1 and 1.5 suns, respectively. Second, the model matched the experimental temperature data to within 1.5 %. Panels A and C were similar.

Table 3. Steady-State Performance at selected evaporator power and lamp power settings.

ANALYSIS (HP Power Loss @ 10%)										
Test #	Lamp Power In (W)	Lamp Power Output (W)	Ave. Test HP Power (W)	HP Power Loss (%)	Ave. Analysis HP Power (W)	RDU Max Temp. (K)	HP T(K) TC#16	Panel T(K) TC # 39	Panel T(K) TC # 25	Panel T(K) TC # 11
1	112	50.0	0.0	10.00%	0.0	267.0	NA	259.9	267.0	259.9
2	150	66.6	0.0	10.00%	0.0	288.2	NA	279.0	288.2	279.0
3	112	50.0	206.0	10.00%	185.4	399.9	399.9	369.3	374.9	369.3
4	112	50.0	300.8	10.00%	270.7	444.0	444.0	398.9	406.2	398.9
5	112	50.0	355.6	10.00%	320.0	467.1	467.1	413.6	422.0	413.6
6	150	66.6	206.9	10.00%	186.2	408.9	408.9	378.3	384.5	378.3
7	150	66.6	301.0	10.00%	270.9	451.1	451.1	406.2	414.1	406.2
8A	150	66.6	346.7	10.00%	312.0	470.0	470.0	418.1	426.8	418.1
8B	150	66.6	346.7	10.00%	312.0	442.4	442.4	394.5	396.2	394.5

Figure 6 shows the temperature gradient observed across the panel with the lamp nodes in the model providing 50 watts each, and no evaporator wattage applied, consistent with the non-uniform distribution of light across the panel as deployed in the thermal vacuum chamber. The span in temperature was modest, a few degrees. With evaporator wattage applied, the temperature gradient across the panel was tens of degrees greater, as shown in Figure 7. The important conclusion to glean from Figures 7 and 8 is that the high thermal conductivity fibers serve to distribute heat across the face sheet and the heat pipes serve to distribute heat along their length, regardless of heat origin. The overall conclusion to draw from the steady-state modeling is that the thermal model was calibrated against the measured results and the model was found to agree to within 1.5 %.

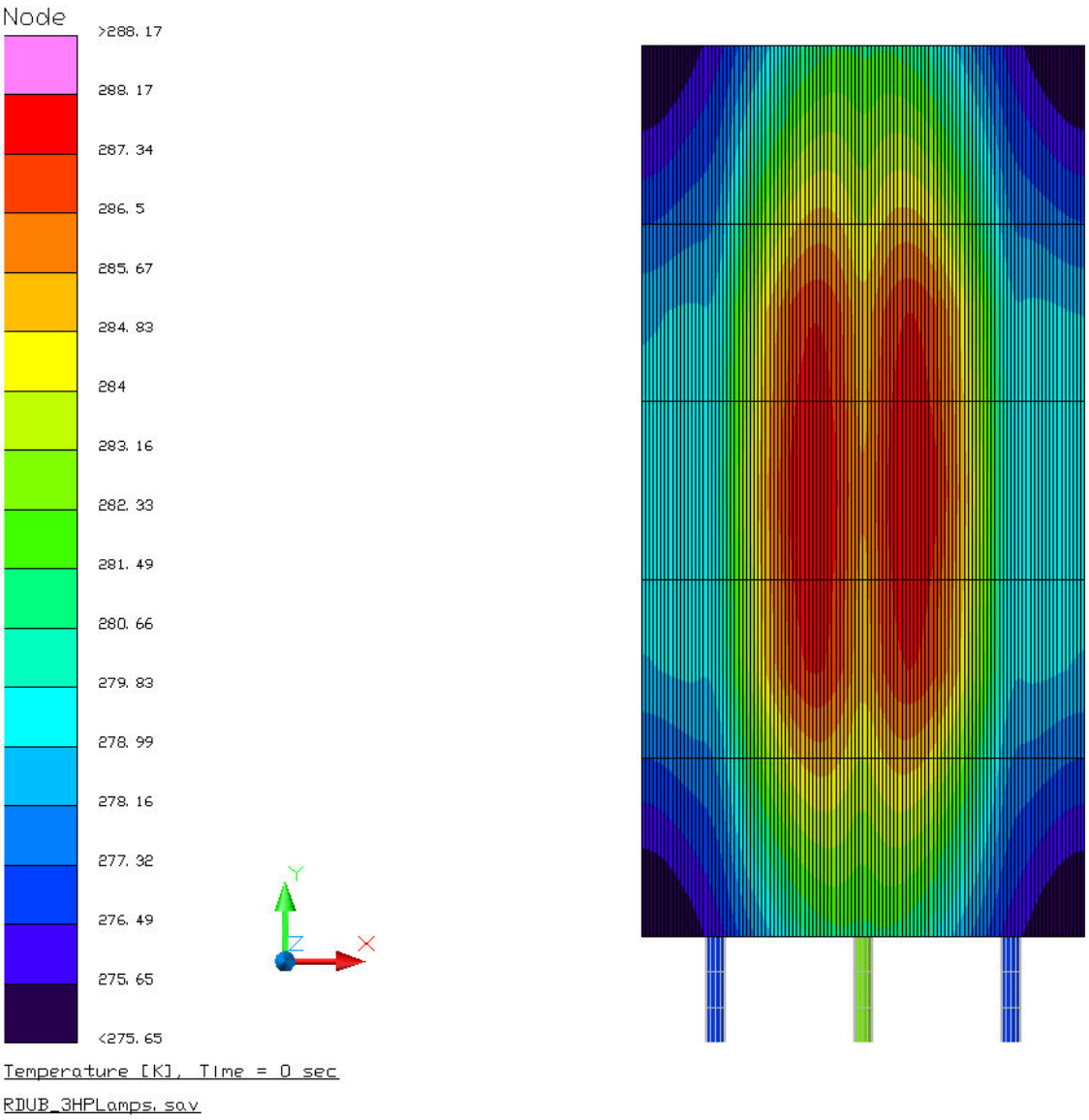

Figure 7. Temperature gradient across the span of the panel with lamps on and no heat applied to the evaporators.

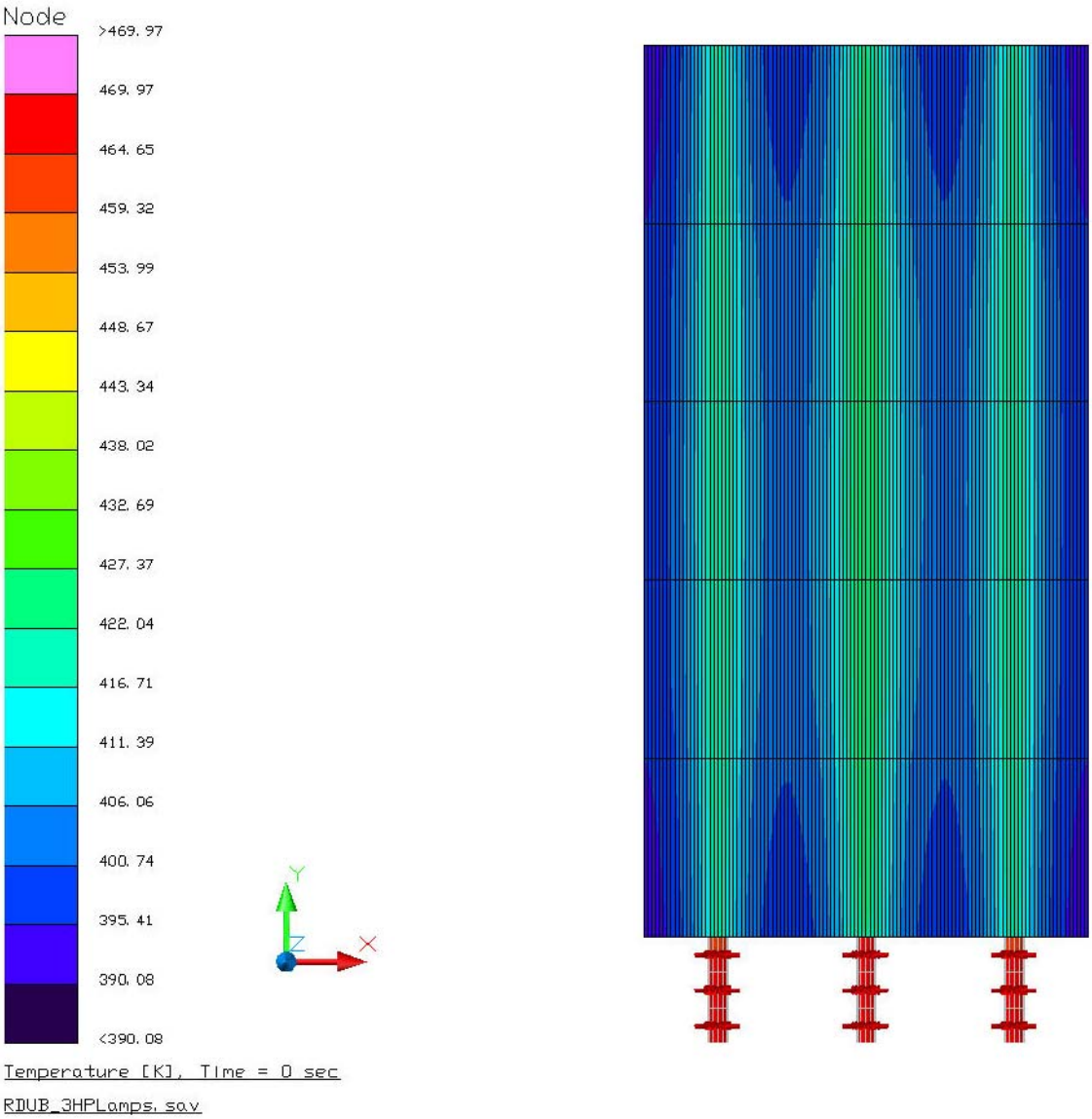

Figure 8. Temperature gradient across the span of the panel with lamps on and heat applied to the evaporators.

B. Laboratory Observations

Steady-state at zero lamp intensity and zero evaporator wattage, under thermal vacuum with the LN2 cold wall operating, was achieved by allowing the panel to cool overnight. Under such conditions, the water in the heat pipes was unmistakably frozen. Given the near-horizontal orientation of the panel within the thermal vacuum chamber, the ice for this test was widely distributed along the interior of the heat pipe within the wick. Upon 1 sun illumination, the panel warmed to approximately 260 K, consistent with the model and insufficient to thaw the ice. Only after adding the first 200 watts of evaporator wattage per heat pipe was there sufficient energy to melt the ice, vaporize the water, and initiate heat pipe operation. Indeed, the transient thermocouple data revealed the progression of vapor down the heat pipe as more and more of the condenser section became active. Another interesting observation was made during transient operation. With a panel composed of three heat pipes, not all three heat pipes came on line together. The thermocouple data as a function of time revealed that heat flow through the high thermal conductivity face sheets served to distribute heat from one heat pipe system to the next. From both the laboratory observations and the steady-state modeling, the data agree that 1 sun illumination of the panel will be insufficient to thaw ice within the heat pipes. Heat pipe operation can only be initiated with added evaporator wattage.

C. First Principles Analysis

Separate from the thermal model discussed above, an additional first principles effort was undertaken to model a vertical radiator panel on the lunar surface at the lunar pole to understand radiator performance during cold soak and initial illumination, in general, and to predict freeze-thaw performance, in particular. This first principles effort to study vertical operation was analysis only. Sink temperatures are defined not only by the surrounding environment but also by the optical properties of the radiator surface in equilibrium with the surrounding environment. The temperature at the lunar surface varies with lunar day.[2] Figure 8 summarizes cold soak temperatures from Reference 2 and shows that coming out of cold soak, the lunar surface temperature is 120 K. The lunar sink temperature for a radiator having the optical properties of a/e = 0.2/0.9 at equilibrium is 230 K.

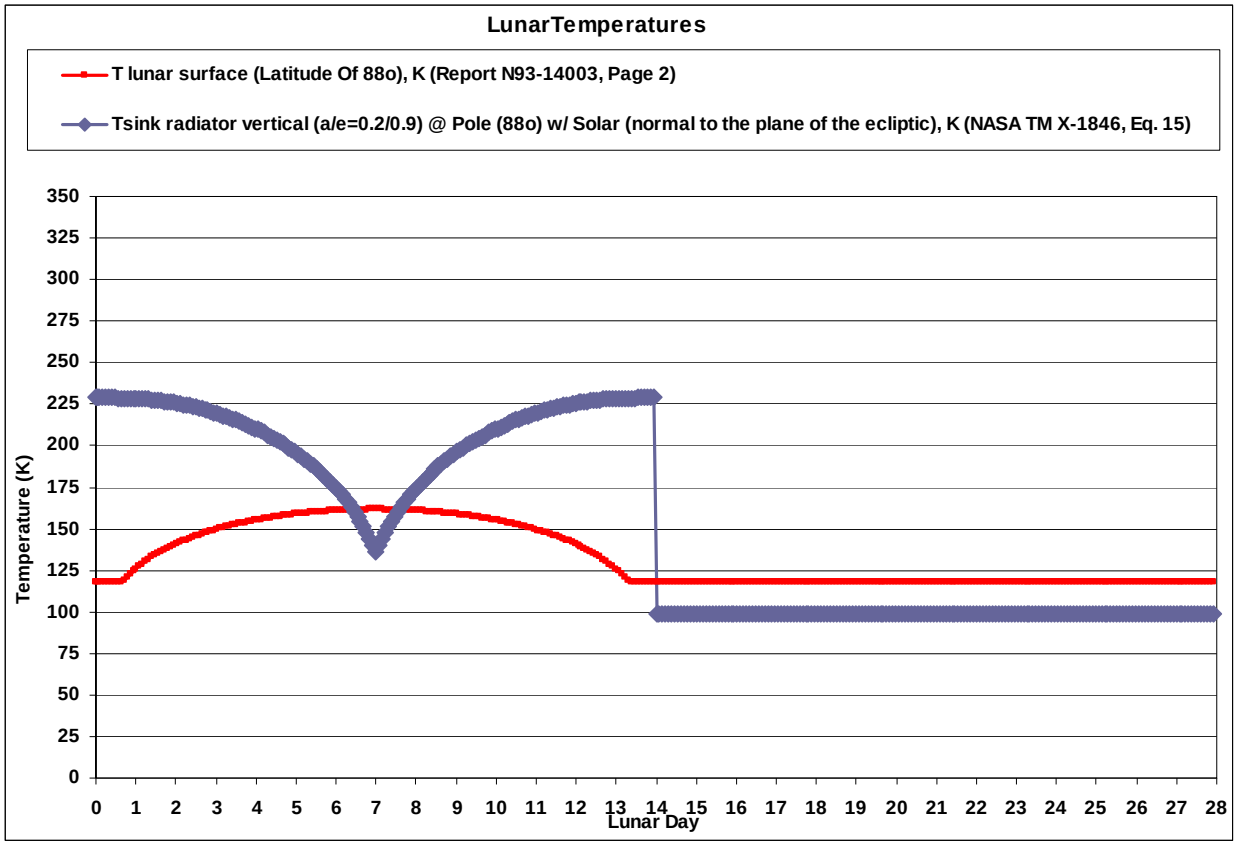

Figure 8. Sink Temperatures at the Lunar Pole as a function of Lunar Day.

The first principles model was utilized to create a transient condition allowing the radiator to come out of cold soak and to be illuminated by one sun on lunar day zero. The result is summarized in Figure 9. At time equal zero, the radiator is at the cold soak condition of 120 K and is illuminated instantaneously. The temperature increases from 120 K to 230 K in about 3600 seconds, the same 230 K expected at equilibrium from Figure 8. The model goes on to create a second transient condition starting at 5000 seconds allowing the radiator to accept heat pipe operation. Once heat pipes are activated, the evaporator temperature climbs quickly to 480 K. The dilemma created by this scenario is that the heat pipes must be above freezing to operate and they are not. Hence, the first principles modeling here agrees with laboratory observations and system level thermal modeling in that the heat pipes will be frozen at lunar sunrise, raises the concern that a radiator coming out of cold soak at lunar sunrise will very quickly reach an equilibrium temperature of 230 K, and that the frozen heat pipes coming out of cold soak at lunar sunrise will require more than 1 sun illumination alone to begin operation.

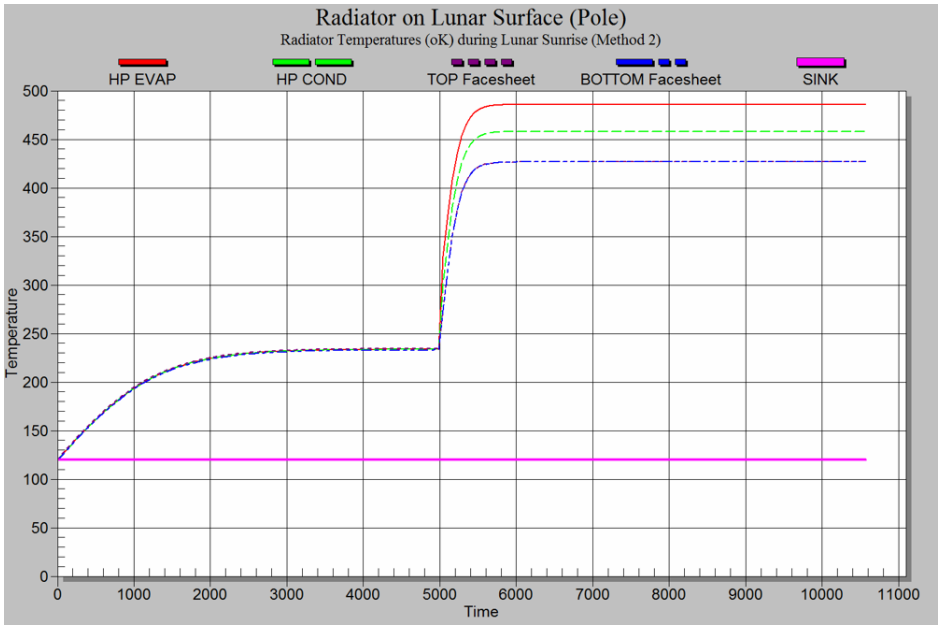

Figure 9. Radiator transient times for a radiator with the optical properties of a/e=0.20/0.90, time in seconds, temperature in Kelvin.

D. Freeze-Thaw Issues

Thermosyphons, heat pipes operating vertically in a gravity field, are charged with a minimum volume of fluid just sufficient to wet the entire wick during optimum operation. Water is selected for its unequalled thermal properties. By selecting titanium as the wall material, there is sufficient strength to prohibit thermal ratcheting and wall damage. Indeed, the water pooled at the bottom of the thermosyphon prior to start up expands axially into the pipe upon freezing and is readily available at the evaporator upon start up. A concern is raised that should ice formation occur in the condenser section of the heat pipe upon cool down, insufficient water would be present in the evaporator to enable subsequent start up. This concern is most prevalent as a result of an unexpected shut down of the radiator, and the concern is an issue at any time.

Another interesting unknown is the consequence of g-forces at launch on the distribution of water in the heat pipes combined with freezing during the lengthy transit to the moon. Launch forces could drive liquid water in the heat pipe to an undesirable location in the minutes after launch, i.e. collecting in the condenser, and the lengthy transit to the moon could freeze the water at that location hampering subsequent start up.

The high thermal conductivity of the face sheet offers the possibility of a cascading start, by starting one heat pipe and allowing heat flow through the face sheet to melt the water in the next heat pipe in line. Once liquid, the vapor front can progress down the length of the pipe heating the face sheet until the next heat pipe in line melts. Such a scheme would require a means to thaw the first heat pipe in line.

E. Future Work

Much future work is planned. At the laboratory scale, a study is now under way to understand heat pipe operation when powered by a closed loop heat source and a variety of heat exchanger configurations. Also planned is a study on thermosyphon operation, including start up, cool down, and various wick configurations, with emphasis on freeze-thaw behavior. System level testing is also planned utilizing a 2nd generation radiator demonstration unit deployed in a vertical orientation in a thermal vacuum chamber.

V. Conclusion

A study was undertaken to evaluate the performance of 1st generation radiator demonstration unit panels operating under 1 sun and 1.5 sun illumination in a thermal vacuum environment. Emphasis was placed on first heating the panel with radiant energy from quartz halogen lamps followed by adding wattage to the panels from cartridge heaters placed around the heat pipe evaporators. Steady-state modeling, laboratory observations, and first principles modeling were included in the study. The steady-state modeling, laboratory observations, and first

principles modeling all revealed that 1 sun illumination was insufficient to thaw ice residing in the heat pipes and that additional evaporator wattage was needed to thaw the ice and initiate heat pipe operation.

Acknowledgments

The authors would like to thank David A. Scheiman, Arctic Slope Research Corporation, for his help in conducting the beam survey and for computing lamp intensity values.

References

1. Jaworske, D.A., Beach, D.E., Sanzi, J.L., "Heat Rejection Systems Utilizing Composites and Heat Pipes: Design and Performance Testing," 5th International Energy Conversion Engineering Conference, St. Louis, MO, AIAA-2007-80969, 2007.

2. Simonsen, L.C., DeBarro, M.J., and Farmer, J.T., "Conceptual Design of a Lunar Base Thermal Control System," The Second Conference on Lunar Bases and Space Activities of the 21st Century, Volume 2, pp 579-591, 1992.

3. Dallas, T., Diaguila, A.T., and Saltsman, J.F., "Design Studies on the Effects of Orientation, Lunation, and Location on the Performance of Lunar Radiators," NASA TM X -1846, 1971.